



Molecular Crystals and Liquid Crystals Science and Technology. Section A. Molecular Crystals and Liquid Crystals

Publication details, including instructions for authors and
subscription information:

<http://www.tandfonline.com/loi/gmcl19>

Structural Behavior and Photochemical Reactivity of Silicone Copolymers with Functional Side Groups

J. M. Buisine ^{a b}, X. Coqueret ^c & C. Lahmamssi ^{a d}

^a Laboratoire de Dynamique et Structure des Matériaux
Moléculaires, U.R.A. CNRS n° 801

^b Equip. de Thermophysique de la Matière Condensée, Université
du Littoral-Quai Freycinet 1, B.P. 5526, F-59379, Dunkerque,
France

^c Equipe de Physique des Stases Anise-tropes, université des
Sciences et technologies de Lille, F59655, Villeneuve d'Ascq,
Cedex, France

^d Laboratoire de Chimie Macromoléculaire, Université des
Sciences et Technologies de Lille, U.R.A. CNRS n° 351, F-59655,
Villeneuve d'Ascq Cedex, France

Version of record first published: 04 Oct 2006.

To cite this article: J. M. Buisine, X. Coqueret & C. Lahmamssi (1996): Structural Behavior and Photochemical Reactivity of Silicone Copolymers with Functional Side Groups, Molecular Crystals and Liquid Crystals Science and Technology. Section A. Molecular Crystals and Liquid Crystals, 281:1, 295-311

To link to this article: <http://dx.doi.org/10.1080/10587259608042253>

PLEASE SCROLL DOWN FOR ARTICLE

Full terms and conditions of use: <http://www.tandfonline.com/page/terms-and-conditions>

This article may be used for research, teaching, and private study purposes. Any substantial or systematic reproduction, redistribution, reselling, loan, sub-licensing, systematic supply, or distribution in any form to anyone is expressly forbidden.

The publisher does not give any warranty express or implied or make any representation that the contents will be complete or accurate or up to date. The accuracy of any instructions, formulae, and drug doses should be independently verified with primary sources. The publisher shall not be liable for any loss, actions, claims, proceedings, demand, or costs or damages whatsoever or howsoever caused arising directly or indirectly in connection with or arising out of the use of this material.

Structural Behavior and Photochemical Reactivity of Silicone Copolymers with Functional Side Groups

J. M. BUISINE^{*a}, X. COQUERET⁺ and C. LAHMAMSSI^{*b}

^{*L} Laboratoire de Dynamique et Structure des Matériaux Moléculaires, U.R.A. CNRS n° 801

^a Equipe de Thermophysique de la Matière Condensée, Université du Littoral-Quai Freycinet 1, B.P. 5526, F-59379 Dunkerque, France

^b Equipe de Physique des Stases Anisotropes, université des Sciences et technologies de lille, F59655 Villeneuve d'Ascq, Cedex, France

⁺ Laboratoire de Chimie Macromoléculaire, U.R.A. CNRS n° 351, Université des Sciences et Technologies de Lille, F-59655 Villeneuve d'Ascq Cedex, France

(Received July 4, 1995; in final form September 29, 1995)

In order to rationalize the peculiar photochemical behavior of some silicone copolymers containing cyanostyrylacrylic (CSA) side groups connected to the main chain through a branched spacer, thermophysical studies including microscopic, calorimetric and diffractometric analysis were conducted. An oligomeric trisiloxane containing the same type of functionality was also studied as a model compound. Although CSA acid and its simple alkyl ester derivatives exhibit only true crystalline order, layered (smectic or crystalline) structure was evidenced for the model compound. The series of reactive polysiloxanes containing various amounts of functional units shows phase separation. The photosensitive esters are gathered with part of the main chains in the ordered microdomains dispersed in a silicone-rich phase. The weight fraction of reactive side groups in the mixed microdomains was determined by calorimetric measurements indicating an almost unchanged composition of the microphases from one polymer to another. Several observations based on bulk state photochemistry showed a leveled reactivity independent of the macroscopic content in photosensitive groups. The layered order observed by wide angle X-ray scattering is consistent with the clean, reversible photoreaction and with the observed kinetics.

Keywords: Polysiloxane, photoreactive polymer, liquid crystal, phase separation.

INTRODUCTION

Solid state photochemistry is a research area particularly rich in opportunities for achieving structure reactivity investigations. Since the development of the basis concepts of topochemistry¹, a number of chromophores giving rise to [2 + 2] photocycloaddition in the crystalline state have been examined in detail². The dimerization of various crystalline forms of cinnamic acid³ is still a subject of current interest.⁴ This basic reaction scheme has been applied to crystalline compounds bearing two reactive groups, thus opening the route to solid state step-growth photopolymerization.⁵ Conversely, the dimerization of cinnamate derivatives as polymer-bound chromophores has proved to be of great industrial interest⁶. Polyvinylcinnamate is the most

representative photopolymer working as a negative resist.⁷ The photoreaction in the glassy polymer matrix has been studied recently.⁸ The reactivity measured at various temperatures suggests the existence of preoriented pairs of chromophores.⁹

Our current interest in photo-cross-linkable silicone polymers has led us to synthesize functional siloxane copolymers including cinnamic or cyanostyrylacrylic (CSA) esters side groups. The previous study¹⁰ relative to the specific photochemical reactivity displayed by these polymers indicated two types of behavior depending on the nature of the photoreactive moieties. The series of polymers containing cinnamic ester side groups are viscous resins exhibiting a reactivity similar in many respects to that of liquid alkyl cinnamates of low molecular weight,¹¹ thus contrasting the behavior of poly(vinylcinnamate) in the glassy state. Isomerization was indeed shown as the most important relaxation process taking place upon UV irradiation of the initially all-trans cinnamates. With polysiloxanes P_{1-4} including CSA pendant groups, the reactivity studied by qualitative and quantitative UV spectroscopy revealed a set of features which, to be understood, require knowledge of the physical structure and morphology of the systems. The present report deals with the thermophysical characteristics of various silicone polymers bearing CSA lateral groups.

2. EXPERIMENTAL PART

2.1. Materials

Cyanostyrylacrylic(CSA) acid (2-cyano-5-phenyl penta-2,4-dienoic acid) was prepared according to the standard procedure.¹² Methyl, butyl, octyl, decyl and dodecyl CSA esters were prepared by reacting the sodium salt of CSA acid with the proper bromoalkane. The esters were purified by recrystallisation from ether-light petroleum solutions. Trisiloxane TS containing a single CSA side group and the analogous copolymers P_{1-4} were synthesised and purified as described in our previous paper.¹³ Some thermophysical characteristics of unfunctionalized silicone copolymers were determined with poly(methylsiloxane-co-dimethylsiloxane) P_0 of a number average degree of polymerization $DP_n = 240$ and containing 7 mol-% of $-\text{[MeHSi-O]}-$ units.

2.2. Methods

Phase sequences, transition properties and phase structures have been studied by three thermophysical analysis methods. Transition temperatures and phase textures have been determined by thermomicroscopy using a polarizing microscope (Leitz) equipped with a heating and cooling stage (FP 52-Mettler). The working range of the standard equipment is of 30 to 250 °C. The temperature was controlled at ± 0.5 °C. The lower temperatures (about -60 °C) were reached with a flow of cold nitrogen gas in a special device developed in our laboratory. To achieve temperature control the maximal cooling rate was -10 °K \cdot min $^{-1}$ between $+20$ °C and -30 °C and was -5 °K \cdot min $^{-1}$ between -30 °C and -60 °C.

The nature – 1st order of glass – of the transformation as determined by differential scanning calorimetry (DSC 7-Perkin Elmer) in the temperature range from -170 °C to $+180$ °C. Heating experiments were performed at 10 to 30 °K \cdot min $^{-1}$. On cooling, the

rates were between 2 and 5 °K · min⁻¹. Temperature control was ± 0.5 °C. For quenching the samples, the cooling rates were about 100 °K · min⁻¹ with no temperature control. Structural studies were performed by diffractometry using a curved detector (CPS 120-INEL) efficient in the angular range from 0 to 120° for 2θ (wavelength λ K_α (Cu) = 1.54 Å). A gas flow cryostat (ENRAF NONIUS) allowed the experiments to be performed between -170 °C and +30 °C. Diffractograms were recorded at constant temperature ± 0.5 °C. Between two experiments the sample was heated at ca. 10 K · min⁻¹. Quenching rates were higher than 40 °K min⁻¹ with uncontrolled temperature.

3. CONDENSED STATE PHOTOREACTIVITY

The qualitative analysis of the UV spectra recorded from thin films submitted to increasing 350 nm light dose indicates that a clean photochemical process takes place. The presence of an isobestic point at 290 nm together with the recovery of the initial optical density at 345 nm upon irradiation with 254 nm UV light (Fig. 1) is reminiscent of the main characteristics of the photoreaction given in the solid state by some crystalline esters of CSA.¹⁴ The dimerization of methyl cyanostyrylacrylate is represented in Scheme 1 as the possible reaction taking place with polymer bound photosensitive groups. Quantitative analysis of the dimerization kinetics indicated that the quantum yield can be expressed by a power law involving the mole fraction of unreacted chromophores α to the power 3:

$$\Phi(\alpha) = \Phi_0 \alpha^3$$

The strong dependence of the quantum yield $\Phi(\alpha)$ upon α is not consistent with hypothetical crystalline packings of chromophores arranged in rows with two nearest neighbors, or by pair, with a single nearest neighbor.¹⁵ These two observations thus suggest the existence of partially ordered structure.

The comparison of the quantum yields of dimerization for the various samples submitted to kinetic analysis showed a surprising independence of the initial value of the quantum yield $\Phi(1) = \Phi_0$ and of the variations of $\Phi(\alpha)$ on the macroscopic average content in functional units. This suggested that the concentration of the reactive groups was leveled from one sample to another, as would be expected from a segregated system.

4. THERMOPHYSICAL STUDIES

4.1. Acid and esters derived from CSA

Optical, calorimetric and diffractometric measurements show that CSA acid as well as the simple esters with C₁, C₄, C₈, C₁₀ or C₁₂ linear alkyl chains do not exhibit mesomorphic behavior. Despite the presence of the aromatic and polar moiety also found in several calamitic liquid crystals, the wide and rigid molecular architecture of these compounds leads to crystalline structures with high melting temperatures.¹⁶ Two crystalline phases were observed for the acid and for the octyl and propenyl esters.

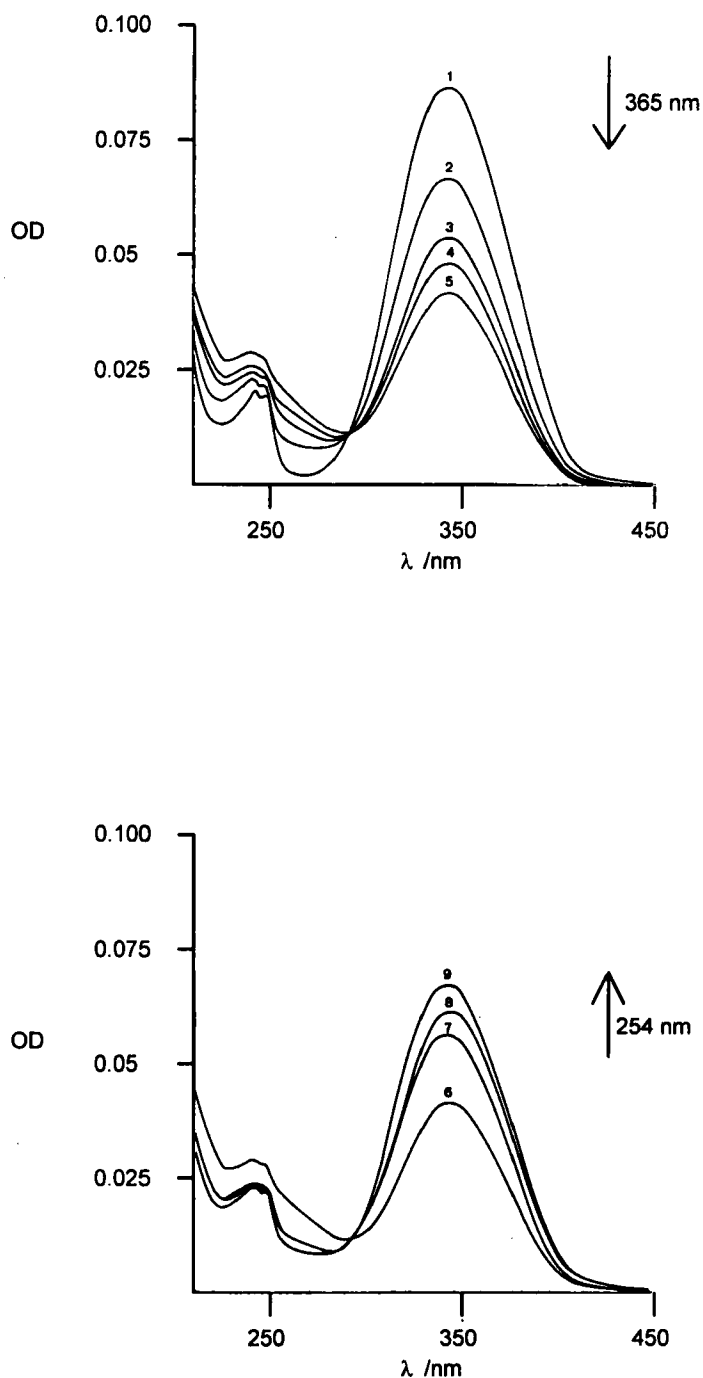
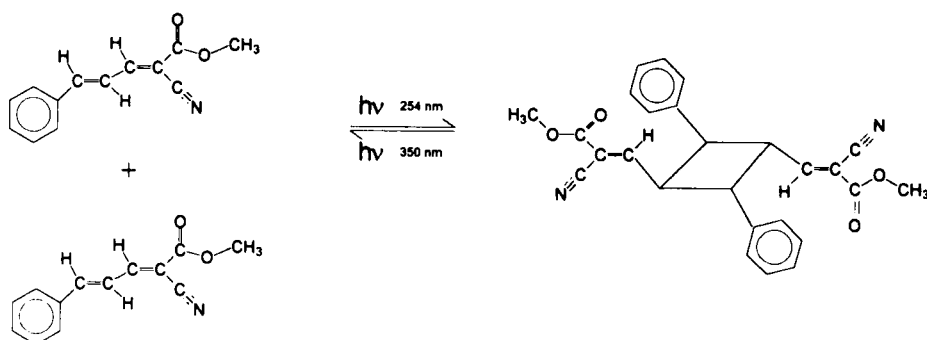


FIGURE 1 Changes in the UV spectra of polymer P_1 submitted to UV irradiation as a thin film cast on a quartz plate: a): dimerization under 365 nm irradiation, curve 1: before irradiation, curve 2: after 10 s, curve 3: after 30 s, curve 4: after 40 s, curve 5: after 90 s; b): retrodimerization under 254 nm irradiation curve 6: before irradiation, curve 7: after 2.5 s, curve 8: after 5 s, curve 9: after 10 s.

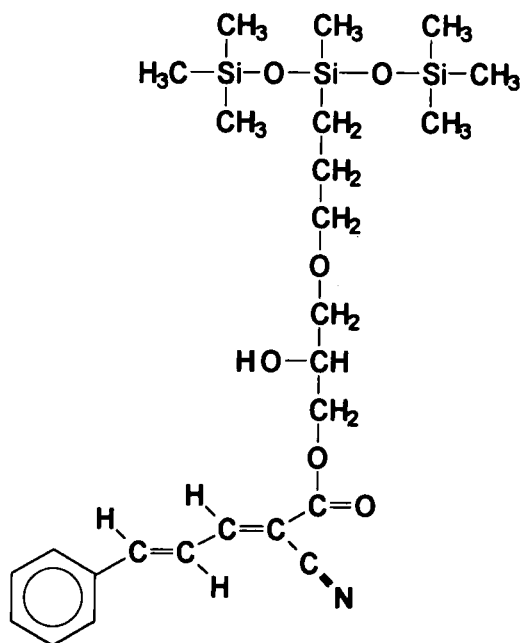


SCHEME 1 Reversible photodimerization of crystalline methyl cyanostyrylacrylate.

4.2. Trisiloxane

Microscopical observations show that model compound TS is in the isotropic liquid state at room temperature. Upon observation during cooling from 100 to -60°C , the compound exhibits at about -30°C a heterogeneous texture with very small bright areas dispersed in a dark matrix. However, it was not possible to observe birefringence for all the sample in spite of several experiments conducted at various slow rates of cooling followed by heating. Keeping the sample at constant low temperature should lead to the growth of the areas, but could not be achieved successfully with our laboratory equipment. On heating they were shown to disappear at -25°C .

Model trisiloxane TS



Selected X-ray diagrams obtained from TS are presented in Fig. 2. Whatever the quenching temperature and cooling rate, the diffractograms obtained at -150°C (Fig. 2a) and at room temperature are quite similar. They exhibit two maxima respectively: a faint one at about $2\theta = 3^{\circ}$ and spread one between $2\theta = 12.5^{\circ}$ and 25° , which are both characteristic of an amorphous structure. Thus, at low temperature, the compound is in a glassy state which is in fact the glassy liquid. The mean transverse distance between molecules, calculated from the angular position of the maximum of the diffuse ray at a large angle is about 4.7 \AA . By reheating, between -50 and -8°C , one can observe

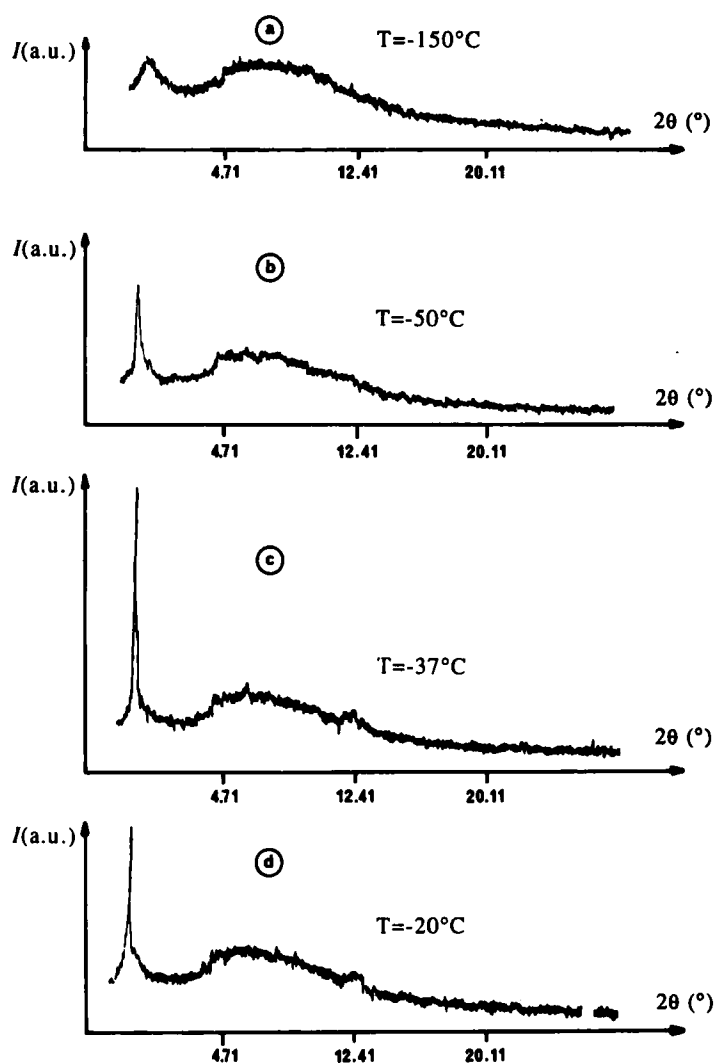


FIGURE 2 Diffractograms from trisiloxane TS: a) by quenching the sample at -150°C from room temperature, b), c) and d) by reheating respectively at -50°C , -37°C and -20°C after quenching.

a superimposed sharp peak at $2\theta = 3^\circ$, the intensity of which is maximum between -37°C and -20°C . Another low intensity peak also appears for $2\theta = 27.5^\circ$ between 37°C and -8°C . By cooling down slowly, both peaks can also be observed. In all cases the peaks can only appear after 5 h relaxation time. The low angle peak corresponds to a layered structure for the molecules. The thickness of the layers (29.4 \AA) is very near the calculated molecular length (29 \AA) and the molecules are almost perpendicular to the layers. The width of the low angle peak is quite equivalent to the resolution of the diffractometer which shows a long range order in the layers. The liquid ring keeps the same angular position as in the liquid state and the planar disorder is bidimensional. The small sharp peak corresponds to an approach distance of about 3.25 \AA .

Figure 3 gives two examples of thermograms obtained for different conditions in cooling the sample. The thermal behavior depends upon whether the sample is quenched at -100°C or quenched at -40°C with one hour annealing at -40°C . However, in each case, experiments performed with $10, 20$ or $30^\circ\text{K}\cdot\text{min}^{-1}$ heating rates do not induce changes in the thermograms. All those drawn from -100°C (with or without quenching or/and annealing) exhibit a glass transition at about -55°C (Fig. 3a), which corresponds to the transformation from glassy to under-cooled isotropic liquid. By heating the samples, it appears as a spread exothermic peak (beginning at about -50°C on Fig. 3a) that corresponds to a transformation into a more ordered state. It is followed by an endothermic one beginning at about -4°C and attributed to the clarification. The corresponding amplitude of the enthalpy changes is quite the same for the two transitions and measured near $4 \text{ J}\cdot\text{g}^{-1}$. Thermograms recorded on cooling ($-0.5^\circ\text{K}\cdot\text{min}^{-1}$) from 20 to -80°C , followed by heating ($+0.5^\circ\text{K}\cdot\text{min}^{-1}$ with or without tempering) never exhibit transformation.

For TS, DSC and X-ray experiments give evidence of a layered structure between about -50°C and $+6^\circ\text{C}$. Such behavior needs quenching at low temperature (-100°C) or annealing (forced in DSC measurements, imposed in X-ray diffraction experiments) at higher temperature (-40°C). This leads to the following

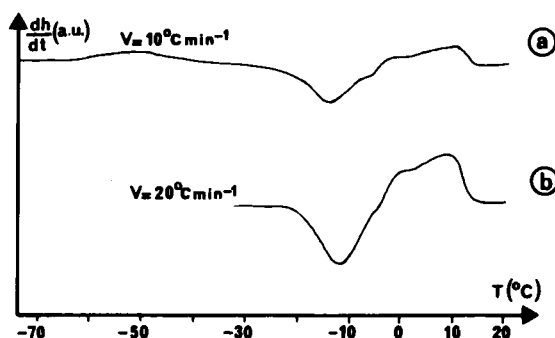
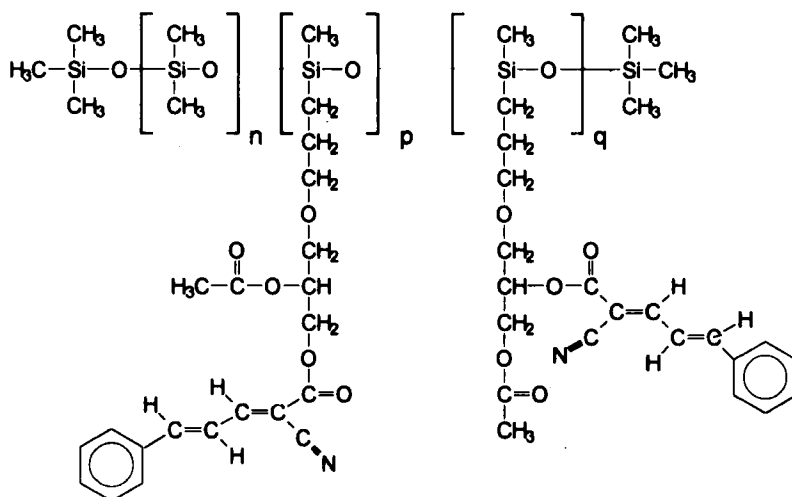


FIGURE 3 Thermograms obtained by heating trisiloxane TS (endothermal changes upwards). a) at $10^\circ\text{K}\cdot\text{min}^{-1}$ after quenching at -100°C , b) at $20^\circ\text{K}\cdot\text{min}^{-1}$ after quenching at -40°C and one hour tempering at -40°C .

phase sequence for increasing temperature under atmospheric pressure: glassy isotropic liquid, undercooled isotropic liquid, layered structure-isotropic liquid. The layered arrangement can be a crystalline or a smectic structure. In the first case, optical observation should reveal the presence of bright areas of crystallites that are actually not observed. We believe that the layered phase can be of the smectic type with very low birefringence and very low kinetic of transformation. The molecular structure of TS is similar to compounds with a disiloxane terminal group recently described in the literature¹⁷. Though the latter exhibit interdigitated layers, the bulky nature of the trisiloxane group in TS probably disrupts packing.

4.3. The Polysiloxanes



The plots of Figure 4 represent schematically the general aspects of thermograms obtained by heating with a $30^\circ\text{K}\cdot\text{min}^{-1}$ rate the polymers quenched at -100°C . They all present the same general features as for the trisiloxane. Other experiments performed with lower heating rates (10 and $20^\circ\text{K}\cdot\text{min}^{-1}$) do not show significant changes in the thermograms. Numerous experiments were performed to obtain accurate data for transformation temperature, and for enthalpy and heat capacity changes.

One glass transition at low temperature is followed by two peaks (the first: endo, the second: exothermic). The temperature and enthalpy change of the endothermic peak can be accurately measured (Table II) on thermograms obtained for samples heated from a temperature slightly lower than room temperature. Both series of data vary in the same and continuous way as the functionalization ratio. Moreover, after quenching at -150°C , thermograms exhibit another glass transition (Fig. 4). The excess of specific heat (see Table II) for the low temperature glass transition (ΔC_{p1}) increases in

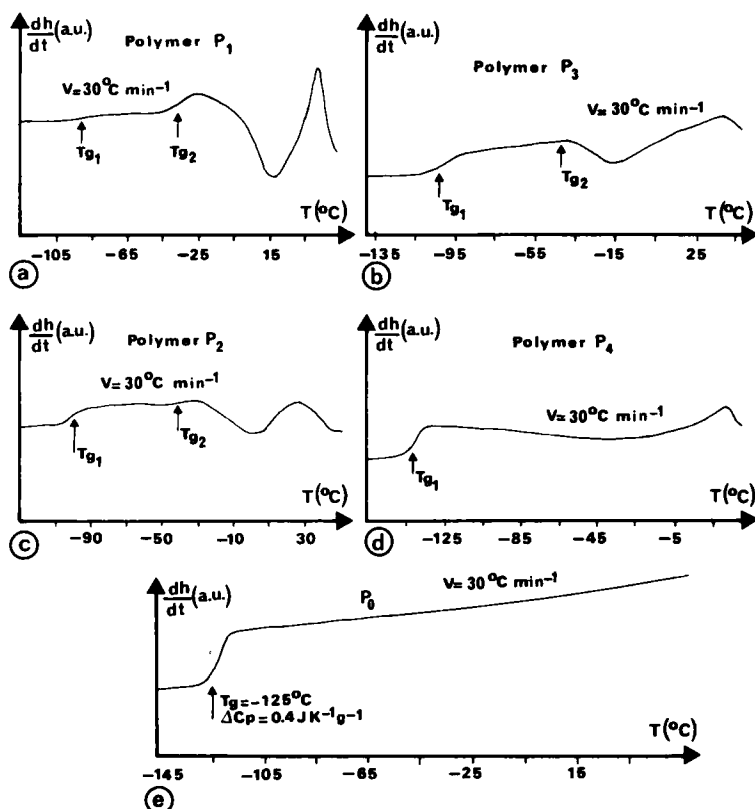


FIGURE 4 Thermograms recorded upon heating functionalized polymers P_{1-4} and the unmodified silicone copolymers P_0 after quenching (endothermal changes upwards).

TABLE I
Structural characteristics and viscosity of the functionalized copolymer.

Polymer	Degree of Polymerization	Mole fraction τ of functionalized repeat unit	Dynamic viscosity at 25 °C (Pa.s)
P_1	33	14.2	4.2
P_2	129	9.5	6.9
P_3	209	7.5	5.7
P_4	241	5.8	9.1

the series of copolymers P_1 to P_4 where the chain length (DP_n) increases and the degree of functionalization τ decreases at the same time. Conversely the specific heat for the high temperature glass transition (ΔC_{p2}) was shown to decrease. Moreover, the low temperature glass transition is not observed for the less functionalized polymer. Other DSC experiments show that poly(dimethylsiloxane-co-methylsiloxane) P_0 , a representative parent polymer without side groups, exhibits a single glass transition at -125 °C

TABLE II

Thermodynamic data of the studied polymers: T_{G_1} and T_{G_2} : glass transition temperature ($^{\circ}\text{C}$), accuracy: $\pm 5^{\circ}\text{C}$, ΔC_{P_1} and ΔC_{P_2} : excess of specific heat at the glass transition ($\text{J}\cdot\text{g}^{-1}\cdot\text{K}^{-1}$), accuracy: $\pm 0.008 \text{ J}\cdot\text{g}^{-1}\cdot\text{K}^{-1}$, ΔH : enthalpy change at the clarification ($\text{J}\cdot\text{g}^{-1}$), accuracy: $\pm 0.2 \text{ J}\cdot\text{g}^{-1}$, T' : clarification temperature obtained by microscopical measurements ($^{\circ}\text{C}$), accuracy: $\pm 0.5^{\circ}\text{C}$, T'' : temperature of the end of clarification obtained by microscopical measurements ($^{\circ}\text{C}$), accuracy: $\pm 0.5^{\circ}\text{C}$.

Polymer	Lower glass transition		Higher glass transition		Clarification	
P_1	T_{G_1}	-90	T_{G_2}	-35	T'	26
					T''	37
	ΔC_{P_1}	0.04	ΔC_{P_2}	0.188	ΔH	8.6
P_2	T_{G_1}	-100	T_{G_2}	-40	T'	25
					T''	36
	ΔC_{P_1}	0.132	ΔC_{P_2}	0.042	ΔH	5.7
P_3	T_{G_1}	-105	T_{G_2}	-45	T'	24.5
					T''	35.5
	ΔC_{P_1}	0.153	ΔC_{P_2}	0.026	ΔH	4.5
P_4	T_{G_1}	-120	T_{G_2}		T'	23
					T''	33
	ΔC_{P_1}	0.215	ΔC_{P_2}		ΔH	33

(Fig. 4). Thus, the glass transition at low temperature (T_{G_1}) which also appears for the photoreactive polymers can be attributed to the main chains that segregate under a pure micro-phase in which the motions are dissociated from those of the side chains.¹⁸⁻¹⁹ The high temperature glass transition (T_{G_2}) is then due to motions of the side groups which are connected to part of the main chains as a mixed microphase. This gives some evidence of a biphasic behavior.²⁰⁻²⁸ The exothermic peak which corresponds to a partial reorganization of the structures is less marked when the sample is cooled slowly (-5 to $20^{\circ}\text{K}\cdot\text{min}^{-1}$) than when it is quenched. This effect can be understood in terms of nucleation and growth competition upon heating and cooling.

Through thermomicroscopic observations at room temperature, the coexistence of birefringent and isotropic domains is observed with textures that are similar for the present series of polymers. Between the crossed polarizer and analyser, birefringent domains are constituted from small disks with dark lines more or less rippled and convergent, dispersed in a dark matrix. Identification or reference to known typical structures was not possible. By heating the sample, the birefringent domains progressively melt over a wide temperature range. Temperatures of the end of clarification are reported in Table II. They vary in the same way as the content in organic side groups. By slow cooling (about $2^{\circ}\text{K}\cdot\text{min}^{-1}$) the extension of the birefringent domains which appears is a function of the functionalization degree τ . Thus, for a given time and a given temperature, the birefringent phase is all the less extended because the functionalization ratio is small. This means that the more important the grafting, the more important the potential of organization. For all the polymers the ordered phase appears and the transformation is complete at about -15°C . It must be noted here that phase separation cannot be observed by microscopical observation because the

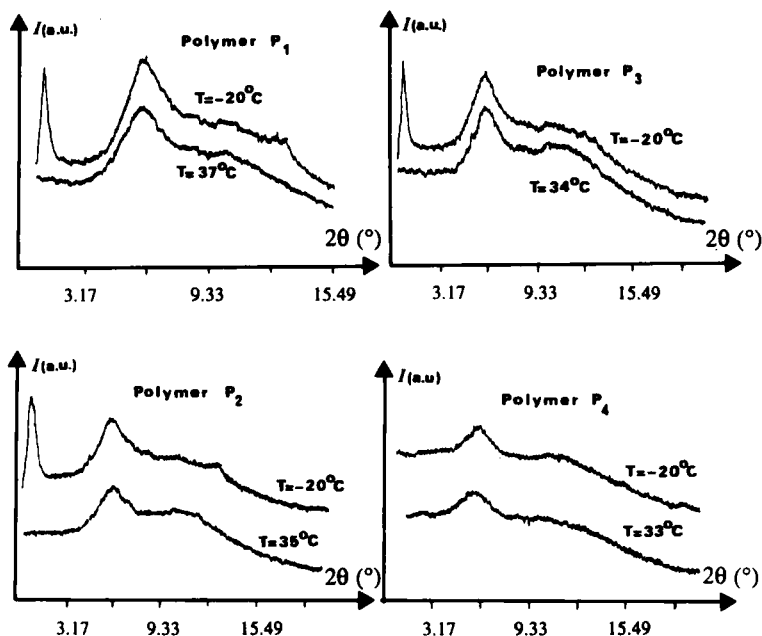


FIGURE 5 Diffractograms obtained from polysiloxanes P_{1-4} at 37°C and at -20°C by reheating after quenching.

size of the microphase domains has the order of magnitude of the chain length (10 to 100 \AA). The phase separation takes place inside the birefringent domains which then include both mixed and pure microphase.

X-ray diffraction patterns recorded at 20°C and above the clarification temperature of the series of photoreactive polymers are collected in Figure 5. In the liquid phase, a spread and intense ray is observed which is maximum at $2\theta = 12^{\circ}$. Spectra obtained after quenching samples at -150°C (not shown here) are also characteristic of an amorphous structure. Thus, at low temperature the compound is in a glassy state which is in fact the glassy liquid. By reheating from the glassy state no change is observed on the X-ray diagrams for P_4 . However, for the three other polymers, the spectra exhibit a sharp peak at $2\theta = 2.4^{\circ}$ and a more or less structured liquid ring which corresponds maximum to that of the liquid phase. By slow cooling from the liquid state, similar X-ray diagrams are obtained. The liquid rings plotted respectively at 37°C and 20°C are well-fitted with a lorentzian curve the characteristics of which are reported in Table III. The correlation lengths are determined using the paracrystal model from mean transverse distance between molecules calculated from the angular position of the maximum of the rays²⁹. The sharp peak at low angle suggests a layered structure. Low angle diffraction measurements give 42 \AA for the thickness of the layers which is higher than the length of the lateral group (30 \AA). Thus, the layers can be considered as formed by lateral rigid groups associated with a 10 \AA layer composed of flexible chains. However, a partially bilayered structure cannot be completely excluded. The intensity

TABLE III

Characteristics of the X-ray spectra obtained for the liquid rings at 37 °C and – 20 °C for the polymers and fitted with lorentzian curves respectively L_1 and L_2 : I : maximal intensity, Q : position of the maximum; ΔQ : width at half height, d : inter-reticular length, L_R : correlation length

Polymer	Type	Channel	$I(\text{a.u.})$	$Q(\text{\AA}^{-1})$	$\Delta Q(\text{\AA}^{-1})$	$d(\text{\AA})$	$L_R(\text{\AA})$
P_1	L_1	580	810	0.85	0.25	7.4	40
	L_2	576	812	0.84	0.20	7.5	50
P_2	L_1	590	627	0.87	0.29	7.2	35
	L_2	580	681	0.85	0.27	7.4	37
P_3	L_1	590	550	0.87	0.32	7.2	31
	L_2	585	550	0.86	0.29	7.3	34
P_4	L_1	594	455	0.88	0.35	7	28

of the low angle peak strongly depends on the functionalization degree of the studied polymer. When τ decreases, the extension of the layered microphases reduces and the organization of the molecules inside the layers decreases so that the low angle peak vanishes for the less functionalized polymer. The lack of longitudinal order can be explained by the very large proportion of the segregated chains. This situation highly affects the dispersed mixed microphase whose layered structure has no chance to appear. This behavior is similar to that of the least functionalized polymers of the other series³⁰. The intensity of the large angle diffuse ring increases with polymerization degree. The liquid ring corresponds to diffusion i) by lateral groups (or transverse order within the layers) ii) by the polymer main chain. The absence of well-marked rays at large angles shows that rigid groups are not ordered inside the layers. However, for P_1 and P_2 there appears a small peak at $2\theta = 25^\circ$ that corresponds to a 4 Å distance and that can be explained by lateral group packing. Mean distances and correlation lengths indicate that the longitudinal and transverse orders only extend to a few molecules, so that there is no long range order. Thus, the more functional the polymer is, the more extended the longitudinal order.

Microphase separation, as it occurs in the polymers, is the reason for the formation of a layered structure. As described for the model compound, the layered arrangement can correspond to a crystalline or a smectic structure of the side groups. To date, no typical liquid crystalline texture could be observed. Further experiments are necessary to determine whether the structure is smectic or not. All the diffractograms exhibit a reflection at 7.4 Å associated with a 35 Å correlation length. It corresponds to the distance between the siloxane layers. After clarification, this reflection is observable, indicating that phase separation is still present to some extent in the isotropic state.^{27–28}

5. DISCUSSION

5.1. Phase Separation

For the polymers, as a consequence of the existence of two glass transitions, a two-phase behavior is deduced.^{20–28} The introduction of lateral groups induces a phase separation in the polymers: a pure microphase, constituted by main chains, co-exists with a mixed microphase, formed from the association of lateral groups and main chains. This phase separation is due to the low compatibility of the flexible silicone parts of the main chain and the rigid and polar lateral groups. These groups aggregate with part of the chains and create microdomains irrespective of the other part of the segregated chains. The values of the weight fraction X_1 for the main chain and X_2 for the side chain in the polymer allow the mode of partition of both species (main chains and side chains) to be determined. On the other hand, from X_1 the excess of heat capacity of the chains in the microphase (without side chains) can be calculated:

$$\Delta C_{p1} \text{ specific for the chain} = \frac{\Delta C_{p1}}{X_1}$$

The ratio between ΔC_{p1} specific and ΔC_p and the uncross-linked polymer gives the fraction x_1 of the main chains that are segregated in the pure microphase. Symmetrically, the fraction x_1 provides the fraction of main chains that are associated with the lateral groups. On the other hand, the values x_1 and x_2 allow the mode of partition of both species in the microphases to be determined. In fact, the proportion of material which appears as main chains in the pure microphase is

$$C_{MC}^{(1)} = x_1 \cdot X_1.$$

The proportion of material which appears as main chains associated (or “dissolved”) with side chains in the mixed microphase is

$$C_{MC}^{(2)} = x_2 \cdot X_1.$$

Assuming that all side chains are in the mixed microphase inducing the high temperature glass transition, the portion of material which appears as side chains in the microphase is

$$C_{LG} = 1 \cdot X_1$$

with

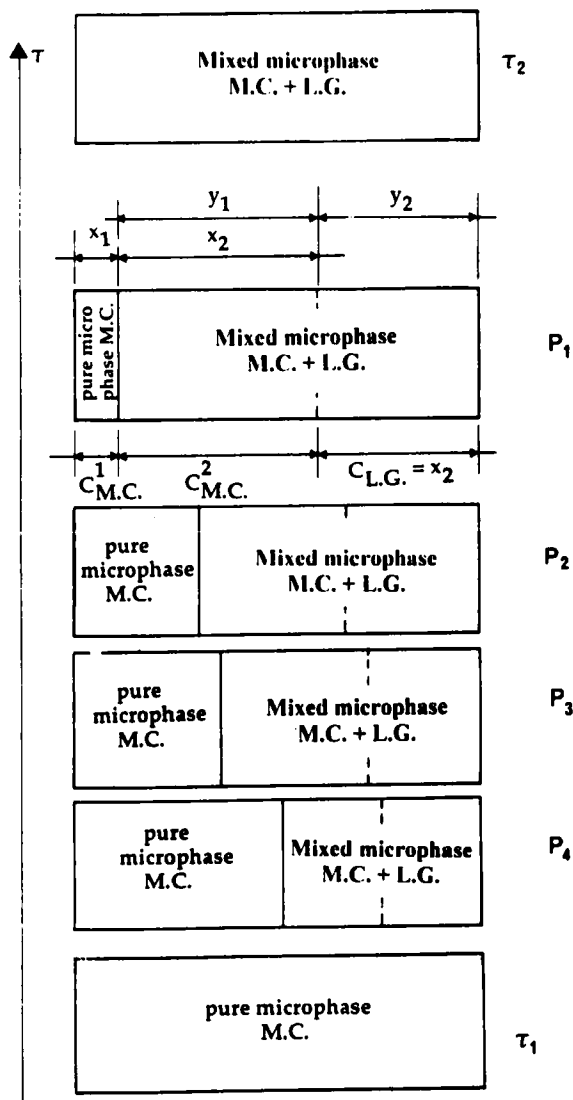
$$C_{MC}^{(1)} + C_{MC}^{(2)} + C_{LG} = 1.$$

All these physico-chemical specifications allow the microphase compositions to be determined, y_1 in main chains and y_2 in lateral groups:

$$y_1 = \frac{x_2 \cdot X_1}{x_2 \cdot X_1 + X_2}$$

$$y_2 = \frac{X_2}{x_2 \cdot X_1 + X_2} \quad \text{with} \quad y_1 + y_2 = 1.$$

Data for X_1 , X_2 , x_1 , x_2 , $C_{MC}^{(1)}$, $C_{MC}^{(2)}$, C_{LG} , y_1 , y_2 are reported in Table IV. The proportion x_1 of the segregated main chains increases when the functionalization degree τ decreases. The proportion of the second phase increases with the content in lateral group one. Thus the introduction of side groups induces phase separation. A schematic representation of the distribution of the two species in the two microphases versus τ for temperatures lower than the clarification zone is given Scheme 2. For the polymers (Scheme 2 b-e), the (intermediate) values of constitutional parameter



SCHEME 2 Schematic representation of the distribution of the two species in the two microphases (M.C.: main chains, L.G.: lateral groups).

TABLE IV

Numerical data for the physico-chemical specifications giving the partition of the main and side chains of the polymers

Polymer	X_1	X_2 $= C_{L.G.}$	x_1	x_2	$C_{M.C.}^1$ $= x_1 X_1$	$C_{M.C.}^2$ $= x_2 X_2$	$y_1 = \frac{x_1 X_2}{x_2 X_1 + X_2}$	$y_2 = \frac{X_2}{x_2 X_1 + X_2}$
P_1	0.603	0.397	0.166	0.834	0.1	0.503	0.558	0.442
P_2	0.686	0.314	0.481	0.519	0.33	0.356	0.531	0.469
P_3	0.734	0.266	0.521	0.479	0.382	0.351	0.568	0.432
P_4	0.781	0.219	0.688	0.312	0.537	0.243	0.525	0.474

τ leads to the dissociation of the system in pure and mixed microphases inducing two glass transitions for the quenched samples. For very high (τ_2) or very low (τ_1) content in lateral groups, one can expect (Scheme 2a and f) a homogeneous system exhibiting at room temperature a mixed smectic microphase or a pure amorphous phase respectively. Although the composition of the mixed microphase remains constant, surprisingly (Table IV), the glass transition temperatures T_{G1} – of the main chain in the pure microphase – and T_{G2} – of the mixed microphase – increase with the content in functional side groups. This can be understood by the mutual dynamic interaction between main chains and lateral groups. Thus, the increase of T_{G1} from P_4 to P_1 can be interpreted by the decrease of the main chain mobility in the pure microphase. This phenomenon can result from topological constraints due to the phase separation that confine anchoring points between lateral groups and main chains at interfaces between

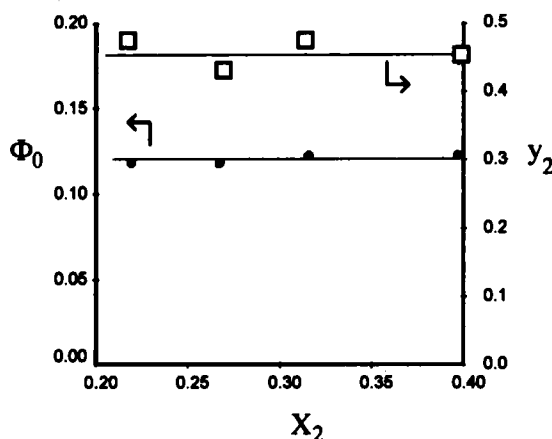


FIGURE 6 Plot of the initial quantum yield of dimerization Φ_0 and of the calculated weight fraction y_2 of CSA ester in segregated microphases as a function of the average macroscopic weight fraction X_2 of CSA esters in polymers P_1 – P_4 in the condensed state.

both phases. This effect is, of course, expected to be strongly dependent on the value of τ since this parameter controls the average length of the dimethylsiloxane segments between two functionalized units.

In the layered microphase, the proportion of main chains is important ($y_1 = 55\%$) and induces disorder. For polymer P_4 , despite the lack of high order at molecular level and microphase level, a certain rough organization of the microdomains induces shape birefringence³¹ which explains the optical anisotropy of the photosensitive polysiloxane.

The peculiar distribution of the photosensitive lateral groups suggested by photoreactivity studies¹⁰ is confirmed by the present thermophysical studies. The loss of photoreactivity as determined by measuring the dimerization rate immediately after heating the polymer samples above the clarification temperature (ca. 45 °C) is in qualitative agreement with the conclusions of the present study. The transition to a homogeneous molten state obviously results in diluting in the silicone rich region in the side groups previously packed in the ordered domains. The observed invariance of the initial quantum yield Φ_0 for various macroscopic concentrations in functional side groups is correlated with the actual concentration y_2 of the dimerizable side groups in the segregated microdomains, as exemplified in the diagram of Figure 6.

6. CONCLUSION

Although CSA acid and its simple alkyl ester derivatives only exhibit crystalline structure, layered (smectic or crystalline) arrangement was evidenced at $-20\text{ }^\circ\text{C}$ for the model compound containing the same type of functionality coupled to an oligomeric trisiloxane. The series of reactive polysiloxanes containing various amounts of functional units shows phase separation. The photosensitive esters are gathered with part of the main chains in the ordered microdomains dispersed in a silicone-rich phase. The weight fraction of reactive side groups in the mixed microdomains was determined by calorimetric measurements. Simple calculation based on the changes of heat capacity allows determination of the composition of the segregated systems observed at room temperature with the various functionalized silicone copolymers. According to this model, the results indicate almost unchanged composition of the segregated microphases from one polymer to another. Several observations based on bulk state photochemistry showed a leveled reactivity independent of the macroscopic content in photosensitive groups. The layered order suggested by WAXS is consistent with the clean, reversible photoreaction and with the observed kinetics. The degree of order in the mixed microphase is expected to be the prime parameter controlling the stereochemistry of the photocycloaddition reaction. The physical characterization indicated only short range order, the nature of which is still under question. The determination of the structure of the photoproducts should afford useful information, as exemplified previously with cinnamic derivatives⁹. Further derivation of the cross linked polymers is currently in progress to allow the stereochemical analysis of the CSA ester dimers.

Acknowledgements

The authors thank Prof. M. More, Dr. C. Gors and Dr. C. Legrand for their help in carrying out some of the experiments and for fruitful discussions.

References

- [1] M. D. Cohen and J. M. G. Schmidt, *J. Chem. Soc.*, 1996 (1964).
- [2] J. M. G. Schmidt, in *Solid State Photochemistry*, D. Ginsburg Ed., Verlag Chemie, Weinheim (1978).
- [3] H. Stobbe and K. Bremer, *J. Prakt. Chem.*, **123**, 1 (1929).
- [4] G. Wegner, *J. Am. Chem. Soc.*, **113**, 1039 (1993).
- [5] M. Hasegawa, *Chem. Rev.*, **83**, 507 (1983).
- [6] L. M. Minsk, J. G. Smith, W. P. Van Deusen and J. F. Wright, *J. Appl. Polym. Sci.*, **2**, 302 (1959).
- [7] D. A. Holden, in *Encyclopedia of Polymer Science and Engineering*, Vol. 11, Wiley, New York, p. 187 (1988).
- [8] A. Reiser and P. L. Egerton, *Macromolecules*, **12**, 670 (1979).
- [9] P. L. Egerton, E. Pitts and A. Reiser, *Macromolecules*, **14**, 95 (1981).
- [10] X. Coqueret, A. El Achari, A. Hajaiej, A. Lablache-Combier, C. Loucheux and L. Randrianarisoa, *Makromol. Chem.*, **192**, 1517 (1991).
- [11] P. L. Egerton, E. M. Hyde, J. Trigg, A. Payne, P. Beynon, M. V. Mijovic and A. Reiser, *J. Am. Chem. Soc.*, **103**, 3859 (1981).
- [12] G. Wittig and R. Kethur, *Chem. Ber.*, **69**, 2079 (1936).
- [13] A. Hajaiej, X. Coqueret, A. Lablache-Combier and C. Loucheux, *Makromol. Chem.*, **190**, 327 (1989).
- [14] H. R. Swamy, V. Ramamurthy and C. N. R. Rao, *Indian J. Chem. Sect. B*, **21B**, 79 (1982).
- [15] G. Desiraju and V. Kannan, *Proc. Indian Acad. Sci.*, **96**, 351 (1986).
- [16] G. W. Gray, in *Molecular Structure and Properties of Liquid Crystals*, Academic Press, London (1962).
- [17] M. Ibn-Elhaj, H. J. Coles, D. Guillon and A. Skoulios, *J. de Phys. II*, **3**, 1807 (1993).
- [18] J. M. G. Cowie, Z. Hag and I. J. Mc Ewen, *J. Polym. Sci., Polym. Lett. Ed.*, **17**, 771 (1979).
- [19] J. M. G. Cowie, Z. Hug, I. J. Mc Ewen and J. Velikovic, *Polymer*, **22**, 327 (1981).
- [20] H. Ringsdorf and A. Schneller, *Br. Polym. J.*, **13**, 43 (1981).
- [21] V. V. Tsukruk, V. V. Schilov, Y. S. Lipatov, I. I. Konstantinov and Y. B. Americk, *Acta Polym.*, **31**, 63 (1982).
- [22] V. V. Schilov, V. V. Tsukruk, V. N. Bliznyuk and Y. S. Lipatov, *Polymer*, **23**, 484 (1982).
- [23] H. Finkelmann and G. Rehage, *Macromol. Chem., Rapid. Commun.*, **3**, 859 (1982).
- [24] R. C. Allen, G. L. Wilkes, I. Yilgor, D. Wu and J. E. Mc Grath, *Makromol. Chem.*, **187**, 2909 (1986).
- [25] C. S. Hsu and V. Percec, *Polym. Bull.*, **17**, 91 (1987).
- [26] C. S. Hsu, and V. Percec, *Makromol. Chem.*, **188**, 331 (1987).
- [27] S. Westphal, S. Diele, A. Mädicke F. Kushel, U. Scheim, K. Rühlmann B. Hisgen and H. Ringsdorf, *Macromol. Chem. Rapid. Commun.*, **9**, 489 (1988).
- [28] F. Kushel, A. Mädicke, S. Diele, U. Utschick, B. Hisgen and H. Ringsdorf, *Polym. Bull.*, **23**, 373 (1990).
- [29] B. K. Vainshtein, "Diffraction of X Rays by Chain Molecules", Elsevier, Amsterdam (1966).
- [30] C. Lahmamssi, J. M. Buisine, N. Isaert, C. Gors and X. Coqueret, *Bull. Pol. Acad. Sci., Chem. Series*, **41**, 267 (1994).
- [31] A. Skoulios, *J. Polym. Sci.: Polym. Symposium*, **58**, 369 (1977).